Published in final edited form as:
J Mol Biol. 2007 January 19; 365(3): 722–731.

Identification and characterization of single chain anti-cocaine catalytic antibodies

Kathleen M. McKenzie, **Jenny M. Mee**, **Claude J. Rogers**, **Mark S. Hixon**, **Gunnar F. Kaufmann**, and **Kim D. Janda***
The Skaggs Institute for Chemical Biology, Departments of Chemistry and Immunology, and The Worm Institute of Research and Medicine, The Scripps Research Institute, La Jolla California, 92037

Summary

Cocaine is a powerful and addictive stimulant whose abuse remains a prevalent health and societal crisis. Unfortunately, no pharmacological therapies exist and therefore alternative protein-based therapies have been examined. One such approach is immunopharmacotherapy, wherein antibodies are utilized to either bind or hydrolyze cocaine thereby blocking it from exerting its euphoric effect. Towards this end, antibodies capable of binding and hydrolyzing cocaine were identified by phage display from a biased single chain antibody library generated from the spleens of mice previously immunized with a cocaine phosphonate transition state analog hapten. Two classes of antibodies emerged based on sequence homology and mode of action. Alanine scanning mutagenesis and kinetic analysis revealed that residues H97, H99, and L96 are crucial for antibodies 3F5 and 3H9 to accelerate the hydrolysis of cocaine. Antibodies 3F1 through 3F4, which are similar to our previously identified 3A6 class of antibodies, catalyze hydrolysis through transition state stabilization by tyrosine or histidine residues H50 and L94. Mutation of either one or both tyrosines to histidine conferred hydrolytic activity on previously inactive antibody 3F4. Mutational analysis of residue H50 of antibody 3F3 resulted in a glutamine mutant with a rate enhancement three times greater than wildtype. A double mutant, containing glutamineH50 and lysineH52, showed a ten-fold rate enhancement over wildtype. These results indicate the power of initial selection of catalytic antibodies from a biased antibody library in both rapid generation and screening of mutants for improved catalysis.

Keywords

cocaine; catalytic antibodies; phage display; immunopharmacotherapy; structure based design

Introduction

Cocaine (**1**, Figure 1) is a powerful and addictive stimulant whose abuse remains a prevalent health and societal crisis. Many medical problems, including death, often accompany cocaine use and the association of the drug with the spread of AIDS is of concern [1,2]. Despite intensive efforts, the development of effective therapies for cocaine craving and addiction remain elusive due to the mode of action of cocaine. Cocaine acts as an indirect dopamine agonist by blocking the dopamine transporter in the pleasure/reward center of the brain [3,4]. Thus, an excess of dopamine builds up in the synapses, leading to an amplification of pleasure sensations. In fact,

*Corresponding author, Email addresses of the corresponding authors: kdjanda@scripps.edu.

due to this difficulty of antagonizing a blocker, there are no effective pharmacological therapies currently available [5]. This difficulty has dictated the need for an alternative strategy to treat cocaine addiction, namely the development and use of protein-based therapies. One approach is to identify a protein that can sequester cocaine, thereby preventing it from reaching brain target areas where it exerts its euphoric effects. Using an immunopharmacological approach, our laboratory [6,7,8,9] and others [10,11], have demonstrated that anti-cocaine antibodies can prevent the psychomotor effects attributable to cocaine. Passive immunization of rats with monoclonal antibody (mAb) GNC92H2 impeded the entry of cocaine into the brain and thus led to a significant decrease in stereotypic behavior [7,8]. In addition, mAb GNC92H2 is capable of blocking cocaine toxicity in an overdose model [9]. Another protein-based approach is to accelerate the hydrolysis of the cocaine benzoyl ester to its corresponding non-psychoactive products methyl ecognine **2** and benzoate (Figure 1). Cocaine is hydrolyzed in this manner in the body by both liver carboxylesterase h-CE2 and butyrylcholinesterase BChE [12,13]. Unfortunately, BChE is three times more effective at catalyzing hydrolysis of biologically inactive (+)-cocaine rather than the naturally occurring (−)-cocaine [14]. Recently, a bacterial cocaine esterase (cocE) was isolated from soil growing the cocaine producing plant *Erythroxylum coca* [15]. Unfortunately, due to the bacterial nature of this enzyme, it is not a viable therapeutic as it would be rapidly cleared via proteolysis and immune surveillance. In addition, this protein is unable to enter the CNS thereby limiting its effectiveness. In addition to these enzymes, catalytic antibodies capable of hydrolyzing cocaine have been identified [16,17,18,19].

Catalytic antibodies have been shown to effectively and selectively catalyze a wide range of reactions, from hydrolysis of esters and amides to pericyclic reactions [20,21]. Traditionally, catalytic antibodies have been generated by mAb technology [22] in which mice are immunized with transition-state analog (TSA) haptens [23,24]. Alternatively, catalytic antibodies may be generated by reactive immunization, in which the hapten undergoes a chemical reaction during immunization, [25], or bait and switch immunization, where a charged hapten elicits a complementary charged residue [26,27]. Several cocaine haptens based upon the proposed transition state of the hydrolysis of the benzoyl ester of cocaine have been previously synthesized [18]. Active immunization of mice with hapten GNL (**3**, Figure 1) linked to the carrier protein KLH led to the identification of several mAbs capable of hydrolyzing cocaine (Table 1) [28,29]. Although antibodies with similar activities have been shown effective in passive immunization studies [30,31], in order to provide a more viable treatment, the kinetic parameters must be improved [18,32]. Both spontaneous [33,34,35] and esterase-catalyzed [13, 34,35,36,37] hydrolysis of cocaine contribute to the short *in vivo* half-life of approximately 30 minutes in human blood. Therefore, for an enzyme or catalytic antibody therapy to be effective, extensive clearance of cocaine must take place within minutes. For a mAb to clear a typical single-dose amount of “steady-state” circulating cocaine (~300 ng/mL, ~5 μM) from the bloodstream within a minute, and a large fraction of the rapid onset, peak arterial levels (~2000 ng/mL) before substantial transit into the brain, we suggest that an administered catalytic mAb circulating at a practical, long-term clinical level of approximately 0.1 mg/mL (~1.5 μM in active sites for whole IgG) must have a minimum $k_{cat}/K_m \sim 10^4\ M^{-1}\ sec^{-1}$ [38].

Typically, two approaches are utilized to improve catalytic constants. One approach is to repeat immunization and hybridoma generation. This allows for a larger sampling of monoclonal antibodies to be analyzed, thereby increasing the chances of identifying an antibody with greater catalytic activity. Unfortunately, this technique is both expensive and laborious, making it inaccessible to most academic laboratories. The second approach involves mutagenesis and affinity maturation of previously identified antibodies. Antibody libraries generated through mutagenesis such as complementarity determining region (CDR) walking and DNA shuffling may then be screened for binding and/or activity by phage display [39,40,41,42]. Phage display is a powerful technique that allows for rapid identification of protein targets of small molecules

through a genotype-phenotype linkage [43,44]. There are reported examples in which six amino acids in a CDR are randomized and then panned by phage display yielding mutants with catalytic activities as much as 12-fold greater than the parent antibodies [45,46].

Herein we report our efforts to probe the specificity and improve the catalytic efficiency of our previously identified antibodies by mutagenesis studies based on the crystal structures of antibodies GNL3A6 and GNL7A1 bound to the phosphonate transition state analog. In addition, we report the identification of new anti-cocaine catalytic antibodies from a biased antibody library synthesized by first immunizing mice with transition state analog GNL followed by panning against the TSA by phage display. The enzymatic properties of these newly identified cocaine hydrolyzing scFv antibodies are reported and catalytic activity is probed by mutagenesis studies.

Results

Expression of GNL antibodies

In order to improve catalysis by mutagenesis, GNL 3A6 and 4D3 were converted to scFv format and cloned into a pETFlag expression vector. Attempts were then made to overexpress soluble scFv in *E. coli*. The use of *E. coli* BL21-gold cells resulted in small amounts of overexpressed protein, with yields ranging from 0.1 to 0.3 mg per liter. We then examined the effect of the concentration of the inducer IPTG on expression and determined that optimal expression was gained with a final concentration of 0.3 mM. However, even with this concentration of IPTG, insufficient protein was obtained for testing the hydrolytic activity of the scFv by HPLC detection of benzoic acid. In examining codon usage, it was determined that there were several residues that relied on rare bacterial codons, therefore we attempted to express the scFv in *E. coli* Rosetta (Novagen), a cell line that contains an additional plasmid encoding for tRNAs for six of the seven rare codons. At the same time we obtained a GNL 3A6 scFv gene in which codon usage was optimized for *E. coli* expression. Expression in Rosetta cells showed no marked improvement and expression with the optimized gene resulted in only slightly better expression (0.3 to 0.5 mg per liter). The poor expression of the optimized clone indicates that this gene may be toxic to *E. coli*. With these attempts unsuccessful, we turned to expression of scFv GNL 3A6 in *Pichia pastoris*, a eukaryotic expression system previously demonstrated to yield large quantities (grams per liter) of scFv antibodies [47]. First, a signal sequence from the yeast alpha mating factor was incorporated C-terminal to the scFv 3A6 gene and this construct was cloned into plasmid pHIL-D2 to allow for expression in *P. Pastoris* GS115 [48]. This construct was grown for 5 days and scFv GNL 3A6 was obtained (approximately 5 mg per liter). Although yeast scFv expression yielded sufficient protein for further studies, this approach was limited by the time involved in expression, thus we turned our efforts towards selection of novel scFvs.

Selection of new scFv GNL binding antibodies

A biased scFv antibody library, in which the heavy chain is linked to the light chain by a $(Gly_4Ser)_3$ linker, was generated using mRNA isolated from the spleens of mice immunized with hapten GNL conjugated to carrier protein KLH. This library was cloned into phagemid vector pCGMT allowing the display of the scFv as a fusion protein on the N-terminus of bacteriophage minor coat protein III [49]. To enrich for antibodies capable of binding to the TSA, the phage library was panned against the GNL-BSA conjugate immobilized on immunotubes. After three rounds of panning and an observed increase in phage titer, ninety-six clones were randomly selected and screened for their ability to bind GNL-BSA by ELISA, using a horseradish peroxidase/anti-M13 conjugated antibody for detection.

Analysis of GNL binding antibodies

Two distinct classes of antibodies emerged from the newly selected clones, antibodies 3F1 through 3F4 and antibodies 3F5 and 3H9. The CDRs are aligned in Figure 2. Antibodies 3F1 through 3F4 are similar to our previously identified GNL3A6 class of antibodies, which includes mAbs GNL 3A6, 4D3, and 7A1. The catalytic activity of this class of antibodies is dependent upon the ability of residues H50 (CDRH2) and L94 (CDRL3) to form an oxyanion hole that stabilizes the transition state through hydrogen bonding (Figure 3) [28]. These two positions are occupied primarily by tyrosine, although antibodies 3F3 and 3A6 contain histidine at one or both of these residues. Finally, in the GNL 7A1 structure, AsnH32 (CDRH1) hydrogen bonds to, and therefore helps stabilize, benzoate after hydrolysis. The other antibodies all contain AspH32, thereby eliminating the hydrogen bonding potential of this residue when deprotonated at neutral pH. Antibodies 3F5 and 3H9 are 89% homologous at the protein level (Figure 2). They are characterized by a short CDRH3 and show the most sequence variation against each other in CDRH2. The only similarities noted with the 3A6 class of antibodies are observed in CDRL1.

The newly selected antibodies were subcloned into a pETFlag expression vector and overexpressed in *E. coli* BL21-gold. Soluble scFvs were tested for their ability to hydrolyze cocaine at a concentration of 20 μM scFv and varying concentrations of cocaine. Benzoic acid concentration was determined by HPLC detection and comparison to a standard curve. The activities of the newly selected antibodies are shown in Table 2. Single chain antibodies 3F1 and 3F4 are incapable of hydrolyzing cocaine, while scFv antibody 3F3 has the greatest catalytic efficiency.

Alanine scanning of scFv 3F5

Since we had no structural information on newly identified scFv 3F5, residues critical for cocaine hydrolysis were determined by alanine scanning mutagenesis. Alanine scanning is a technique in which single residues are mutated to alanine and the mutants are tested for activity. A loss in activity indicates that a residue plays a critical role in the activity of the scFv. Initial efforts were focused on CDRH3 since it is considerably shorter than previously identified antibodies (see Figure 2). We then focused on residues in CDRH2 that vary significantly with scFv 3H9 as well as examining residues capable of hydrogen bonding in CDRH3. Three residues are critical for cocaine hydrolysis: GlnH97, HisH99, and HisL96 (Table 3). Interestingly, these two antibodies show the most sequence variation against each other in CDRH2, yet these differences have had no effect on activity.

Mutational analysis of the oxyanion hole

Using CDR sequence comparisons and crystal structure data from the GNL3A6 class of antibodies, a mutational analysis of residues H50 and L94 was undertaken (Figure 3). Point mutants were constructed, overexpressed in *E. coli*, affinity purified and their catalytic activity was tested by HPLC detection of benzoic acid (Table 4). Comparison of scFv 3A6 and 3F3 Michaelis-Menton kinetics shows that they have the same catalytic rate, yet 3F3 has a 4-fold lower K_m. The difference in these antibodies is that 3A6 has two histidines at positions H50 and L94 where 3F3 only has histidine at position H50. Thus, a 3F3 mutant in which TyrL94 was changed to histidine was tested, and resulted in lower k_{cat} and a greater K_m than the parent antibody. Antibody 3F4 contains tyrosines at both these positions and has no detectable activity. Interestingly, mutation of either residue to histidine, or both residues to histidine, restores the catalytic activity of this antibody.

A series of scFv 3F3 H50 mutants, in which all of the mutants retain the ability to hydrogen bond to the transition state, were examined for their ability to hydrolyze cocaine. A tyrosine mutant catalyzes cocaine hydrolysis 2-fold greater than wildtype. Mutating the histidine to

glutamine improves k_{cat} 3-fold and has a rate enhancement (k_{cat}/k'_{uncat}) of 745. Unfortunately, both of these mutants have K_m values 3 times greater than wildtype, thus the improvement in k_{cat} is exactly offset by a worsening K_m. A double mutant that contains this glutamine and mutates arginine H52 to lysine has a catalytic activity greater than 7-fold over wildtype and a rate enhancement of 2040. The K_m of this antibody is significantly higher than the wildtype (2.5 mM vs. 0.3 mM) again mutually offsetting kinetic parameters. Mutants H50 arginine and H50 asparagine have no detectable activity.

Discussion

Although previously identified monoclonal antibodies that catalyze cocaine hydrolysis have been demonstrated useful in preventing psychomotor effects attributable to cocaine exposure [18], attempts to increase the catalytic efficiency of these antibodies have proven laborious due to the inability to overexpress adequate quantities of protein for cocaine hydrolysis assays. In addition, to screen large libraries of antibodies, these mAbs must first be converted to either fragment antigen binding (Fab) or scFv format. In this conversion, antibody stability is decreased through the loss of constant regions and this typically translates to a decrease in catalytic efficiency [50]. This effect is observed with GNL3A6 where the mAb has a rate enhancement of 1360 while that of the scFv is 5-fold lower. In addition, *E. coli* utilize a specific subset of codons for gene expression that are different than those employed in mice [51]. Since the original mAb is murine derived, antibody codon usage may not be optimized for bacterial expression leading to translation problems. While it may be possible to circumvent this obstacle by expressing the antibody in a cell line that contains a plasmid encoding for the rare codons, such as Rosetta, we were unable to overexpress adequate quantities of any of the GNL3A6 class of antibodies in this manner. Additionally, a codon optimized scFv 3A6 clone gave inefficient overexpression. These two results indicate that these murine proteins may be toxic to *E. coli* when overexpressed in large quantities therefore ultimately effecting overexpression.

To identify novel catalytic antibodies capable of hydrolyzing the benzoyl ester of cocaine, we decided to utilize selection against the transition state analog GNL by panning a biased scFv phage library. Our laboratory has used this approach on two previous occasions to identify antibodies capable of amide bond hydrolysis and glycosidic bond cleavage [52,53]. The key to the success of identification through phage display was the use of a biased phage library. This library was generated from mice immunized with the transition state analog hapten. Thus rather than scanning a general immune repertoire, the original library is enriched for antibodies against the TSA. The use of phage display for initial identification also allowed several advantages. Perhaps the most important of which is that any newly identified scFvs are inherently capable of expression in bacteria. Although still murine in origin, they will not be selected if they are not amenable to *E. coli* expression. In addition, the positive clones are already in a scFv format that allows for rapid generation of large libraries of mutants for screening of improved catalysis. Although scFvs do have an inherent disadvantage due to instability, conversion of a suitable catalyst to Fab or IgG format should provide an increase in activity.

Using phage display, we were able to identify six new antibodies capable of binding cocaine transition state analog GNL. Four of these antibodies also showed catalytic activity. The new antibodies can be subdivided into two classes based on sequence homology; scFvs 3F1 through 3F4 and scFvs 3F5 and 3H9. Antibodies 3F1 through 3F4 are homologous with our previously identified antibodies GNL3A6, 4D3 and 7A1. It has been observed that catalytic antibodies generated by the same hapten exhibit considerable sequence homology in their complementarity determining regions [54].

Not only are antibodies 3F3 and scFv 3A6 similar in sequence, they have the same catalytic efficiencies (Table 4). Although these antibodies are analogous to those previously identified, the ability to express these scFvs in bacteria provides a means for improvement of catalytic activity by directed evolution techniques. We were able to utilize these new antibodies to examine the ability of tyrosine versus histidine in residues H50 and L94 of the oxyanion hole (Figure 3). Antibody 3F4 contains residues TyrH50 and TyrL94 but is incapable of hydrolyzing cocaine. Mutants with either one or both of these residues changed to histidine gave this scFv detectable catalytic activity. On the other hand, an antibody with two histidines is not necessarily ideal. Antibody 3F3 contains HisH50 and TyrL94 and has an activity similar to scFv 3A6 in which both residues are histidine. Mutating the 3F3 TyrL94 to histidine yielded an antibody with two histidines, decreased catalytic activity while also decreasing binding affinity as evidenced by an increased K_m. Finally, 3F3 HisH50 was mutated to tyrosine, yielding an antibody with two tyrosines, that is, similar to 3F4. Rather than diminishing activity, this antibody has a catalytic activity two-fold greater than the wildtype antibody, however this antibody also had decreased affinity for cocaine. This data suggests that there is no obvious advantage to histidine over tyrosine, although histidine is capable of conferring hydrolytic activity on antibody 3F4, previously shown to merely bind cocaine.

Further analysis of position H50 in antibody 3F3 indicates that other hydrogen bond donating residues can stabilize the negatively charged transition state. A glutamine mutant yields an antibody with a rate enhancement three-fold greater than the wildtype. The catalytic efficiency of this antibody is similar to the wildtype due to an increase in binding affinity. The greatest rate enhancement has been observed with a double mutant at positions H50 and H52. Wildtype residue H52 is an arginine that helps to encapsulate the transition state analog in the active site of the enzyme [28]. Mutating ArgH52 to lysine, along with the HisH50 glutamine mutation, yields an antibody with a rate enhancement of 2040, ten-fold greater than wildtype scFv. In addition, this rate enhancement is greater than our previously identified IgG GNL3A6. Unfortunately, there is currently no kinetic data published for single chain anti-cocaine catalytic antibodies with which to compare this rate enhancement. Previously identified mAb 15A10 was converted to scFv format and mutants were examined, however only relative kinetic data was reported [55].

Antibodies 3F5 and 3H9 represent novel anti-cocaine catalytic antibodies. Although they are 89% homologous, antibody 3F5 is twice as active as antibody 3H9. They are characterized by a short CDRH3 and a majority of the differences between them come from CDRH2. Preliminary alanine scanning of antibody 3F5 has led to the identification of three residues that are crucial for activity; GlnH97, HisH99, and HisL96. Heavy chain residue H99 may provide the difference in activity of the two antibodies. Antibody 3F5 contains a histidine at this position whereas antibody 3H9 contains a tyrosine. This would be parallel to the examples of the 3A6 class of antibodies.

Analysis of previously identified esterolytic catalytic antibodies has revealed similarities in oxyanion stabilization [55,56]. Among antibodies raised against phosphonate or phosphonamidate transition state analogs, the side chains of residues H33, H35 and ArgL96 as well as the backbone amide of residue H96 form the oxyanion hole. Residue H33 is either a tyrosine or asparagine and position H35 is a highly conserved histidine. Cocaine hydrolytic mAb 15A10 is similar with residues AsnH33, TyrH35 and TrpL96 contributing four hydrogen bonds to oxyanion stabilization [55]. Newly identified antibody 3F5 is also dependent upon residue L96 for activity. Antibody D2.3 varies from this theme and oxyanion stabilization results from hydrogen bonding residues AsnL34, TrpH95 and TyrH100D [57]. Antibodies GNL 3A6 and 7A1 appear to be unique in their activity and utilize the side chains of H50 and L94 to stabilize the transition state. These residues are conserved as either tyrosine or histidine. Bacterial esterase cocE has the greatest cocaine hydrolytic activity to date. This enzyme is a

classic serine esterase with an oxyanion hole formed by a tyrosine and a backbone NH [58]. This analysis reveals that amongst these esterolytic antibodies, similar residues including tyrosine, histidine and asparagine, have evolved as the main residues involved in oxyanion stabilization.

Using phage display, we have identified single chain antibodies capable of hydrolyzing cocaine. Four of the antibodies are similar to those previously identified in our laboratory and comparison with the crystal structure of GNL7A1 allowed for mutational analysis of the ability of the residues in the oxyanion hole to stabilize the transition state. One double mutant, scFv 3F3 HisH50Gln, ArgH52Lys, had a marked rate enhancement over wildtype and provides a new starting point for improvement of catalytic efficiency. Two antibodies, 3F3 and 3H9, provided novel sequences and their catalytic residues were determined by alanine scanning mutagenesis. The identification of these residues, GlnH97, HisH99 and HisL96, provides a basis for future structural analysis. Mutagenesis of residues critical for activity and CDR walking followed by library screening by phage display against the transition state analog GNL could provide novel clones with increased catalytic efficiency.

Finally, amongst cocaine catalysts, cocE has the greatest catalytic efficiency to date. The crystal structure of cocE reveals that the active site is located at the bottom of a cleft, thus burying the cocaine within the enzyme [58] while the crystal structure of antibody GNL7A1 reveals only a shallow binding pocket [28]. This is presumably due the fact that hapten GNL is linked off the methyl ester which is on the same face as the benzoyl ester (Figure 1), thus preventing burial of the reactive moiety. In order to achieve catalytic efficiency in an antibody that is comparable to that of cocE, it may be necessary to overcome this limitation by generation of a new hapten for immunization, in which the linker is attached to the opposite end of the molecule leaving the phosphonate free to tunnel into the active site.

Materials and Methods

Bacteria and plasmids

Escherichia coli XL1-Blue electroporation-competent cells (Stratagene) were used for phage expression. *E. coli* BL21-Gold(DE3) (Stratagene) and Rosetta (Novagen) competent cells were used for over-expression of soluble protein. Phage display vector pCGMT[49] was used for construction of the phage library. Soluble scFvs were expressed in pETFlag (derived from pET-15b, Novagen).

Single chain library construction

Total RNA was purified from the spleens of three mice that had been hyperimmunized with the GNL-KLH bioconjugate (RNA isolation kit, Stratagene). First-strand cDNA was synthesized from the above total RNA using a first-strand cDNA synthesis kit (Pharmacia) with a Not I-$(dT)_{18}$ primer. For V_H gene amplification, twenty five separate PCR reactions were prepared using one of 25 different MVH primers and an equimolar mixture of 4 MJH primers. For V_κ genes, twenty five separate PCR reactions were prepared using one of 25 different MVK primers or 3A6EE primer and an equimolar mixture of 4 MLJ primers. Typically, PCR reactions were performed in 20 μl volumes containing 0.5 μL of cDNA, 1 μl each of 0.1 μg/μl primer, 200 μM dNTPs, and 0.4 μl RedTaq polymerase (Sigma). The program is as follows: 4 min of denaturation at 94 °C, followed by 6 cycles of 40 sec at 94 °C, 40 sec at 40 °C, 2 min at 72 °C, followed by 24 cycles of 40 sec at 94 °C, 40 sec at 45 °C, 2 min at 72 °C, terminated by 10 min at 72 °C. After PCR, all V_H and V_κ fragments were agarose gel purified, recovered (Qiagen) and ultimately combined to form two pools, V_H and V_κ. The scFv genes were generated by assembly of V_H and V_κ through a $(Gly_4Ser)_3$ linker sequence. First, equimolar amounts of V_H fragments and V_κ fragments were assembled by PCR without primers in which the overlapping linker sequences drove the hybridization of the various

fragments. An initial denaturation of 4 min at 94 °C was followed by 10 cycles of 40 sec at 94 °C, 30 sec at 45 °C, 50 sec at 72 °C and terminated by 10 min at 72 °C in the absence of primers. After adding the outer primers MVHSfi and MLJSfi, 6 cycles of 40 sec at 94 °C, 40 sec at 40 °C, 2 min at 72 °C, followed by 24 cycles of 40 sec at 94 °C, 40 sec at 45 °C, 2 min at 72 °C were performed. The scFv genes were digested with *Sfi* I (Roche), agarose gel purified, and ligated into the phage display vector pCGMT. The ligation products were electroporated into *E. coli* XL1-Blue cells. After electroporation, cells were plated on Luria-Bertani broth (LB) medium (supplemented with 100 μg/ml carbenicillin and 10 μg/ml tetracycline) in 10 15-cm dishes (Nunc) and incubated overnight at 37 °C. The clones were scraped off the plates into 2YT medium (containing 100 μg/mL carbenicillin and 10 μg/ml tetracycline) and 10 % glycerol and frozen at −80 °C.

Rescue of scFv-displaying phage

To rescue scFv-displaying phage, 200 ml of 2YT medium (supplemented with 100 μg/ml carbenicillin and 10 μg/ml tetracycline) was inoculated with 1.5 ml of cells from the frozen glycerol stock. This culture was then shaken at 37 °C until an OD_{600} reached about 0.6, and 10^{10} colony-forming units of VCSM13 helper phage (Stratagene) were added. After 30 min incubation at room temperature, the culture was shaken for 90 min at 37 °C. Subsequently, kanamycin (70μg/ml) and isopropyl-D-thiogalactoside (IPTG) (1.0 mM) were added and the culture was shaken overnight at 30 °C. Phage particles were purified by precipitation with 4% PEG-8000 and 3% sodium chloride. ScFv-displaying phage was resuspended in phosphate buffered saline, pH 7.4 (PBS).

Panning of scFv library against GNL-BSA

The library was subjected to three rounds of panning. Immunotubes (Maxisorb, Nunc) were coated overnight at 4 °C with 1 ml of GNL-BSA (1:500 in PBS). After blocking with 4 ml of Blotto (4% BLOT-QuikBloting Membrane Blocking in PBS, Chemicon International) for 1 hour at 37 °C, 10^{12} colony-forming unit phage particles in 1 ml PBS were added and incubated for 1 hour at 37 °C. The immunotubes were washed 2 × 4 ml PBS/0.05% Tween20 followed by washing with 2 × 4 ml distilled water. Bound phage were eluted by adding 1 ml of 0.1 M glycine, pH 2.7. Eluted phage were amplified by infection of fresh *E. coli* XL1-Blue cells and the phage rescued as outlined above.

Phage ELISA

A half-area 96-well high binding capacity ELISA plate (Corning, #3690) was coated with 50 μl GNL-BSA (1:500 in PBS) and incubated overnight at 4 °C followed by blocking with Blotto for 1 hour at 37 °C. Typically, 25 μl phage and 25 μl Blotto were added to each well and incubated at 37 °C for 1 hr. After washing, 50 μl of a 1/500 dilution of horseradish peroxidase/anti-M13 conjugate (Amersham Pharmacia) in Blotto was added and incubated at 37 °C for 1 hour. The plate was developed with TMB (3,3′,5,5′-tetramethylbenzidine) substrate (Pierce) and quenched with an equal volume of 2 M H_2SO_4. The absorbance was read on an ELISA plate reader at 450 nm.

Preparation of scFv

The scFv gene fragments were digested with *Sfi* I (Roche), ligated into the expression vector pETFlag, and transformed into *E. coli* DH5α cells. DNA sequencing was used to confirm the correct sequences. For expression, the pETFlag-scFv DNA was transformed into *E. coli* BL21-gold cells. The scFv expression was induced by growth in Teriffic Broth (TB, Invitrogen) containing 0.3 mM IPTG overnight at 30 °C. The Flag-tagged scFvs were purified on anti-Flag M2 affinity agarose (Sigma). The yield of purified scFv in pETFlag varied between 0.5 and 1.5 mg/liter. The purified scFv was dialyzed into PBS, pH 7.4 (Cambrex) overnight at 4 °C

and the protein was subsequently concentrated using an Amicon 10,000 MWCO Membrane (Millipore).

Pichia expression

The scFv 3A6 gene was first mutated using a QuikChange Site-Directed Mutagenesis kit (Stratagene) to eliminate an *Eco*RI restriction site and then amplified with primers introducing a C-terminal signal sequence from the yeast alpha mating factor and *Eco*RI restriction sites. The gene was digested with *Eco*RI and ligated into vector pHIL-D2. This vector was then digested with either NotI or StuI and electroporated into *P. pastoris* GS115. Individual clones were selected from each digestion and the DNA was isolated and amplified to identify whether the clone contained the scFv 3A6 gene. A 1 L culture in BMGY medium was grown overnight at 37 °C followed by centrifugation. The yeast were resuspended in 6 × 500 ml BMMY medium and grown at 28 °C for 5 days. Methanol was added every day to a final concentration of 0.5%. The Flag-tagged scFv was purified on anti-Flag M2 affinity agarose (Sigma). The yield of purified scFv in pETFlag varied between 0.5 and 1.5 mg per liter. The purified scFv was dialyzed into PBS, pH 7.4 (Cambrex) overnight at 4 °C and the protein was subsequently concentrated using an Amicon 10,000 MWCO Membrane (Millipore).

Point mutants and alanine scanning

Point mutant and alanine scanning genes in vector pETFlag were prepared using a QuikChange Site-Directed Mutagenesis kit (Stratagene). For expression, the pETFlag-scFv DNA was transformed into *E. coli* BL21-gold cells. The scFv expression was induced by growth in Teriffic Broth (TB, Invitrogen) containing 0.3 mM IPTG overnight at 30 °C. The Flag-tagged scFvs were purified on anti-Flag M2 affinity agarose (Sigma). The yield of purified scFv in pETFlag varied between 0.5 and 1.5 mg/liter. The purified scFv was dialyzed into PBS, pH 7.4 (Cambrex) overnight at 4 °C and the protein was subsequently concentrated using an Amicon 10,000 MWCO Membrane (Millipore).

Kinetic Experiments

Initial rates of scFv catalyzed degradation of cocaine were determined by monitoring the formation of benzoic acid (BzOH) by analytical reversed-phase HPLC (Hitachi L-7200; Vydac 201TP54 C-18 column; isocratic mobile phase of 14% MeCN, 86% H_2O (0.1% TFA); 1.0 ml min^{-1} flow rate; detection at 254 nm). The retention times for BzOH, benzoyl ecognine, and cocaine were 14 min, 10 min and 20 min, respectively. All experiments were conducted at ambient temperature in PBS, pH 7.4 (Cambrex) with 20 μM scFv and 0.1–4 mM cocaine. The total volume of all reactions was 200 μl. Experiments were performed by adding the appropriate volume of a 40 mM cocaine solution to a solution of scFv in PBS. Four samples containing various concentrations of cocaine (0.1–4 mM) were run simultaneously. An aliquot from each sample was removed for analysis every 200 min via autosampler. The concentration of benzoic acid was determined by interpolation of peak height and area relative to standard curves. Initial rates were calculated by linear regression analysis of plots of [benzoic acid] versus time. The kinetic parameters k_{cat} and K_m were calculated by fitting plots of initial rate versus cocaine concentration to the Michaelis-Menten equation using GraFit Version 5 software (Erithacus Software).

Nucleotide Sequences

The nucleotide sequences for have been deposited with GenBank Data Libraries. scFv 3F1, GenBank accession no. **DQ849033**, scFv 3F2, GenBank accession no. **DQ8490334**, scFv 3F3, GenBank accession no. **DQ849035**, scFv 3F4, GenBank accession no. **DQ849036**, scFv 3F5, GenBank accession no. **DQ849037**, and scFv 3H9, GenBank accession no.**DQ849038**.

Acknowledgements

We wish to thank Tobin J. Dickerson for thoughtful insight and helpful discussion. This work was supported by grants from The National Institutes of Health (DA08590, K.D.J., and DA15700, K.D.J.). K.M.M. was supported by a Ruth Kirschstein National Research Service Award from The National Institutes of Health (DA18024).

References

1. Des Jarlais DC, Friedman SR. AIDS and i.v. drug use. Science 1989;245:578. [PubMed: 2762809]
2. Brody SL, Slovis CM, Wrenn KD. Cocaine-related medical problems: consecutive series of 233 patients. Am J Med 1990;88:325–31. [PubMed: 2327419]
3. Ritz MC, Lamb RJ, Goldberg SR, Kuhar MJ. Cocaine receptors on dopamine transporters are related to self-administration of cocaine. Science 1987;237:1219–23. [PubMed: 2820058]
4. Withers NW, Pulvirenti L, Koob GF, Gillin JC. Cocaine abuse and dependence. J Clin Psychopharmacol 1995;15:63–78. [PubMed: 7714230]
5. Mendelson JH, Mello NK. Management of cocaine abuse and dependence. N Engl J Med 1996;334:965–72. [PubMed: 8596599]
6. Carrera MR, Ashley JA, Parsons LH, Wirsching P, Koob GF, Janda KD. Suppression of psychoactive effects of cocaine by active immunization. Nature 1995;378:727–30. [PubMed: 7501020]
7. Carrera MR, Ashley JA, Zhou B, Wirsching P, Koob GF, Janda KD. Cocaine vaccines: antibody protection against relapse in a rat model. Proc Natl Acad Sci U S A 2000;97:6202–6. [PubMed: 10823960]
8. Carrera MR, Ashley JA, Wirsching P, Koob GF, Janda KD. A second-generation vaccine protects against the psychoactive effects of cocaine. Proc Natl Acad Sci U S A 2001;98:1988–92. [PubMed: 11172063]
9. Carrera MR, Trigo JM, Wirsching P, Roberts AJ, Janda KD. Evaluation of the anticocaine monoclonal antibody GNC92H2 as an immunotherapy for cocaine overdose. Pharmacol Biochem Behav 2005;81:709–14. [PubMed: 16005948]
10. Fox BS, Kantak KM, Edwards MA, Black KM, Bollinger BK, Botka AJ, French TL, Thompson TL, Schad VC, Greenstein JL, Gefter ML, Exley MA, Swain PA, Briner TJ. Efficacy of a therapeutic cocaine vaccine in rodent models. Nat Med 1996;2:1129–32. [PubMed: 8837612]
11. Kantak KM, Collins SL, Lipman EG, Bond J, Giovanoni K, Fox BS. Evaluation of anti-cocaine antibodies and a cocaine vaccine in a rat self-administration model. Psychopharmacology (Berl) 2000;148:251–62. [PubMed: 10755738]
12. Stewart DJ, Inaba T, Tang BK, Kalow W. Hydrolysis of cocaine in human plasma by cholinesterase. Life Sci 1977;20:1557–63. [PubMed: 17804]
13. Dean RA, Christian CD, Sample RH, Bosron WF. Human liver cocaine esterases: ethanol-mediated formation of ethylcocaine. Faseb J 1991;5:2735–9. [PubMed: 1916095]
14. Zhan CG, Zheng F, Landry DW. Fundamental reaction mechanism for cocaine hydrolysis in human butyrylcholinesterase. J Am Chem Soc 2003;125:2462–74. [PubMed: 12603134]
15. Bresler MM, Rosser SJ, Basran A, Bruce NC. Gene cloning and nucleotide sequencing and properties of a cocaine esterase from Rhodococcus sp. strain MB1. Appl Environ Microbiol 2000;66:904–8. [PubMed: 10698749]
16. Landry DW, Zhao K, Yang GX, Glickman M, Georgiadis TM. Antibody-catalyzed degradation of cocaine. Science 1993;259:1899–901. [PubMed: 8456315]
17. Yang GXQ, Chun J, Arakawa-Uramoto H, Wang X, Gawinowicz MA, Zhao Z, Landry DW. Anti-cocaine catalytic antibodies: A synthetic approach to improved antibody diversity. J Am Chem Soc 1996;118:5881–5890.
18. Matsushita M, Hoffman TZ, Ashley JA, Zhou B, Wirsching P, Janda KD. Cocaine catalytic antibodies: the primary importance of linker effects. Bioorg Med Chem Lett 2001;11:87–90. [PubMed: 11206477]
19. Cashman JR, Berkman CE, Underiner GE. Catalytic antibodies that hydrolyze (−)-cocaine obtained by a high-throughput procedure. J Pharmacol Exp Ther 2000;293:952–61. [PubMed: 10869397]
20. Lerner RA, Benkovic SJ, Schultz PG. At the crossroads of chemistry and immunology: catalytic antibodies. Science 1991;252:659–67. [PubMed: 2024118]

21. Schultz PG, Lerner RA. From molecular diversity to catalysis: lessons from the immune system. Science 1995;269:1835–42. [PubMed: 7569920]
22. Kohler G, Milstein C. Continuous cultures of fused cells secreting antibody of predefined specificity. Nature 1975;256:495–7. [PubMed: 1172191]
23. Tramontano A, Janda KD, Lerner RA. Catalytic antibodies. Science 1986;234:1566–70. [PubMed: 3787261]
24. Pollack SJ, Jacobs JW, Schultz PG. Selective chemical catalysis by an antibody. Science 1986;234:1570–3. [PubMed: 3787262]
25. Wirsching P, Ashley JA, Lo CH, Janda KD, Lerner RA. Reactive immunization. Science 1995;270:1775–82. [PubMed: 8525366]
26. Janda KD, Weinhouse MI, Schloeder DM, Lerner RA, Benkovic SJ. Bait and switch strategy for obtaining catalytic antibodies with acyl-transfer capabilities. J Am Chem Soc 1990;112:1274–1275.
27. Shokat KM, Leumann CJ, Sugasawara R, Schultz PG. A new strategy for the generation of catalytic antibodies. Nature 1989;338:269–71. [PubMed: 2922053]
28. Zhu X, Dickerson TJ, Rogers CJ, Kaufmann GF, Mee JM, McKenzie KM, Janda KD, Wilson IA. Complete reaction cycle of a cocaine catalytic antibody at atomic resolution. Structure 2006;14:205–16. [PubMed: 16472740]
29. Isomura S, Hoffman TZ, Wirsching P, Janda KD. Synthesis, properties, and reactivity of cocaine benzoylthio ester possessing the cocaine absolute configuration. J Am Chem Soc 2002;124:3661–8. [PubMed: 11929256]
30. Briscoe RJ, Jeanville PM, Cabrera C, Baird TJ, Woods JH, Landry DW. A catalytic antibody against cocaine attenuates cocaine's cardiovascular effects in mice: a dose and time course analysis. Int Immunopharmacol 2001;1:1189–98. [PubMed: 11407313]
31. Mets B, Winger G, Cabrera C, Seo S, Jamdar S, Yang G, Zhao K, Briscoe RJ, Almonte R, Woods JH, Landry DW. A catalytic antibody against cocaine prevents cocaine's reinforcing and toxic effects in rats. Proc Natl Acad Sci U S A 1998;95:10176–81. [PubMed: 9707620]
32. Meijler MM, Matsushita M, Wirsching P, Janda KD. Development of immunopharmacotherapy against drugs of abuse. Curr Drug Discov Technol 2004;1:77–89. [PubMed: 16472221]
33. Garrett ER, Seyda K. Prediction of stability in pharmaceutical preparations XX: stability evaluation and bioanalysis of cocaine and benzoylecgonine by high-performance liquid chromatography. J Pharm Sci 1983;72:258–71. [PubMed: 6842378]
34. Cunningham KA, Lakoski JM. The interaction of cocaine with serotonin dorsal raphe neurons. Single-unit extracellular recording studies. Neuropsychopharmacology 1990;3:41–50. [PubMed: 2137698]
35. Stewart DJ, Inaba T, Lucassen M, Kalow W. Cocaine metabolism: cocaine and norcocaine hydrolysis by liver and serum esterases. Clin Pharmacol Ther 1979;25:464–8. [PubMed: 428191]
36. Boyer CS, Petersen DR. Enzymatic basis for the transesterification of cocaine in the presence of ethanol: evidence for the participation of microsomal carboxylesterases. J Pharmacol Exp Ther 1992;260:939–46. [PubMed: 1545406]
37. Liu Y, Budd RD, Griesemer EC. Study of the stability of cocaine and benzoylecgonine, its major metabolite, in blood samples. J Chromatogr 1982;248:318–20. [PubMed: 7174764]
38. Evans SM, Cone EJ, Henningfield JE. Arterial and venous cocaine plasma concentrations in humans: relationship to route of administration, cardiovascular effects and subjective effects. J Pharmacol Exp Ther 1996;279:1345–56. [PubMed: 8968359]
39. Winter G, Griffiths AD, Hawkins RE, Hoogenboom HR. Making antibodies by phage display technology. Annu Rev Immunol 1994;12:433–55. [PubMed: 8011287]
40. Raag R, Whitlow M. Single-chain Fvs. Faseb J 1995;9:73–80. [PubMed: 7821762]
41. Barbas CF 3rd, Kang AS, Lerner RA, Benkovic SJ. Assembly of combinatorial antibody libraries on phage surfaces: the gene III site. Proc Natl Acad Sci U S A 1991;88:7978–82. [PubMed: 1896445]
42. Griffiths AD, Duncan AR. Strategies for selection of antibodies by phage display. Curr Opin Biotechnol 1998;9:102–8. [PubMed: 9503596]
43. Rodi DJ, Makowski L. Phage-display technology--finding a needle in a vast molecular haystack. Curr Opin Biotechnol 1999;10:87–93. [PubMed: 10047512]

44. Smith GP. Filamentous fusion phage: novel expression vectors that display cloned antigens on the virion surface. Science 1985;228:1315–7. [PubMed: 4001944]
45. Takahashi-Ando N, Kakinuma H, Fujii I, Nishi Y. Directed evolution governed by controlling the molecular recognition between an abzyme and its haptenic transition-state analog. J Immunol Methods 2004;294:1–14. [PubMed: 15604011]
46. Fujii I, Fukuyama S, Iwabuchi Y, Tanimura R. Evolving catalytic antibodies in a phage-displayed combinatorial library. Nat Biotechnol 1998;16:463–7. [PubMed: 9592396]
47. Ridder R, Schmitz R, Legay F, Gram H. Generation of rabbit monoclonal antibody fragments from a combinatorial phage display library and their production in the yeast Pichia pastoris. Biotechnology (N Y) 1995;13:255–60. [PubMed: 9634767]
48. Yang K, Basu A, Wang M, Chintala R, Hsieh MC, Liu S, Hua J, Zhang Z, Zhou J, Li M, Phyu H, Petti G, Mendez M, Janjua H, Peng P, Longley C, Borowski V, Mehlig M, Filpula D. Tailoring structure-function and pharmacokinetic properties of single-chain Fv proteins by site-specific PEGylation. Protein Eng 2003;16:761–70. [PubMed: 14600206]
49. Gao C, Lin CH, Lo CH, Mao S, Wirsching P, Lerner RA, Janda KD. Making chemistry selectable by linking it to infectivity. Proc Natl Acad Sci U S A 1997;94:11777–82. [PubMed: 9342313]
50. Glockshuber R, Malia M, Pfitzinger I, Pluckthun A. A comparison of strategies to stabilize immunoglobulin Fv-fragments. Biochemistry 1990;29:1362–7. [PubMed: 2110478]
51. Jana S, Deb JK. Strategies for efficient production of heterologous proteins in Escherichia coli. Appl Microbiol Biotechnol 2005;67:289–98. [PubMed: 15635462]
52. Janda KD, Lo LC, Lo CH, Sim MM, Wang R, Wong CH, Lerner RA. Chemical selection for catalysis in combinatorial antibody libraries. Science 1997;275:945–8. [PubMed: 9020070]
53. Gao C, Lavey BJ, Lo CH, Datta A, Wentworth P Jr, Janda KD. Direct selection for catalysis from combinatorial antibody libraries using a boronic acid probe: primary amide bond hydrolysis. J Am Chem Soc 1998;120:2211–2217.
54. Miyashita H, Hara T, Tanimura R, Tanaka F, Kikuchi M, Fujii I. A common ancestry for multiple catalytic antibodies generated against a single transition-state analog. Proc Natl Acad Sci U S A 1994;91:6045–9. [PubMed: 8016113]
55. Larsen NA, de Prada P, Deng SX, Mittal A, Braskett M, Zhu X, Wilson IA, Landry DW. Crystallographic and biochemical analysis of cocaine-degrading antibody 15A10. Biochemistry 2004;43:8067–76. [PubMed: 15209502]
56. Golinelli-Pimpaneau B. Structural diversity of antibody catalysts. J Immunol Methods 2002;269:157–71. [PubMed: 12379360]
57. Charbonnier JB, Golinelli-Pimpaneau B, Gigant B, Tawfik DS, Chap R, Schindler DG, Kim SH, Green BS, Eshhar Z, Knossow M. Structural convergence in the active sites of a family of catalytic antibodies. Science 1997;275:1140–2. [PubMed: 9027317]
58. Turner JM, Larsen NA, Basran A, Barbas CF 3rd, Bruce NC, Wilson IA, Lerner RA. Biochemical characterization and structural analysis of a highly proficient cocaine esterase. Biochemistry 2002;41:12297–307. [PubMed: 12369817]

Abbreviations

mAb
: monoclonal antibody

IgG
: immunoglobulin

Fab
: fragment antigen-binding antibody

scFv
: single chain variable fragment antibody

CNS

central nervous system

KLH

keyhole limpet hemocyanin

CDR

complementarity determining region

TSA

transition state analog

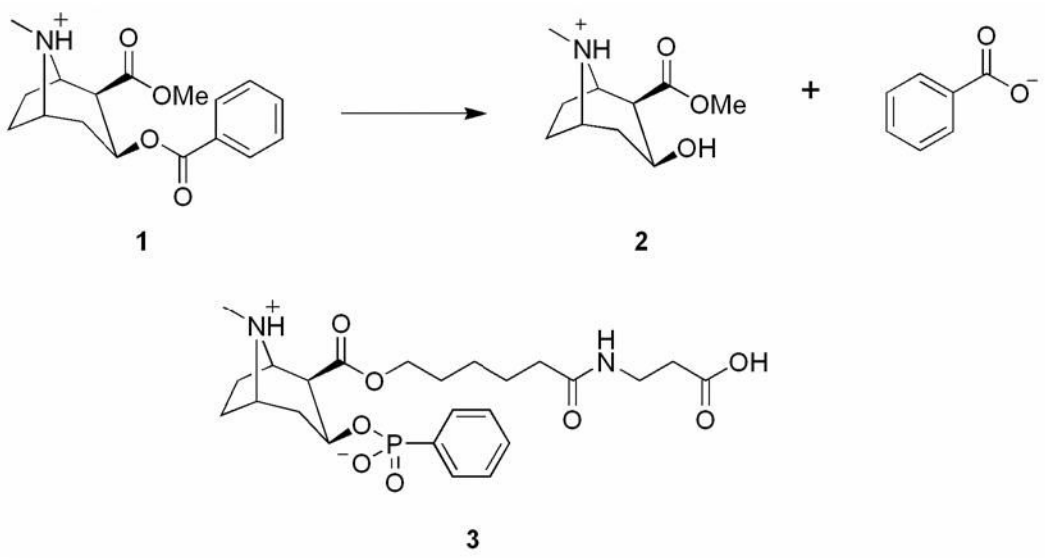

Figure 1.
Hydrolysis of the benzoyl ester of cocaine (1). Transition state analog hapten GNL (3).

A

Ab	CDR1	CDR2	CDR3
3A6*	R**D**YAWT	**H**IRTSGITVYNPSVRS	YEYDGPG--Y
3F1	S**D**YAWT	**Y**IRSSGITRYNPSLKS	YHYFGSS--Y
3F2	S**D**YAWT	**Y**IRNSGTTRYNPSLKS	YHYYGSS--S
3F3	S**D**YAWT	**H**IRNSGITRYNPSLKS	YHYYGSS--Y
3F4	S**D**YAWT	**Y**IRYSAGTRYNPSLKS	YHYYGSS--H
7A1*	**-N**YAWT	**Y**IRSSVITRYNPSLKS	YDYYGNTGDY
3F5	RSYMY-	YIDPYNGDTQNSQRFR	TG**Q**A**H**-----
3H9	NYYMY-	YVDLNYGGSGYNQKFK	TG**Q**A**Y**-----

B

Ab	CDR1	CDR2	CDR3
3A6*	RSSRSLLYKDGRTYLN	LMSTRAS	QQFVD**H**PFT
3F1	RSSKSLLYKDGKTYLN	LMSTRAS	QQFVD**Y**PFT
3F2	RSSKSLLYKDGKTYLN	LMSTRAS	QHFVE**Y**PFA
3F3	RSSKSLLYKDGKTYLN	LMSTRAS	QQFVE**Y**PFT
3F4	RSSKSLLYKDGKTYLN	LMSTRAS	QQFVD**Y**PFT
7A1*	RSSRSLLYKDGRTYLN	LMSTRAS	QQFVE**Y**PFT
3F5	KSSQSLLYSDGKTYLN	LVSKLDS	AQGTHLP**H**T
3H9	KSSQSLLYSDGKTYLN	LVSKLDS	VQGTHLP**H**T

Figure 2.

Alignment of complementarity determining regions. *A*, alignment of heavy chain CDRs. *B*, Alignment of light chain CDRs. *Black*, 3A6 class of antibodies; *blue*, 3F5 and 3H9; *bold*, important residues; (*), previously identified antibodies 3A6 and 7A1, included for comparison. Sequences aligned with Vector NTI (Informax).

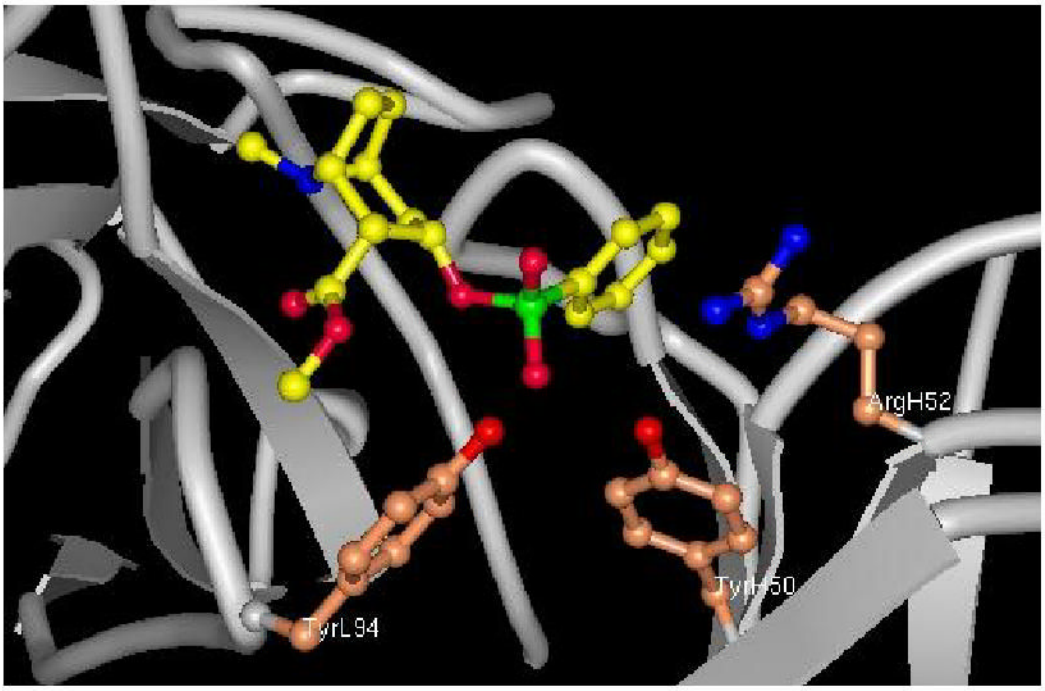

Figure 3.
GNL transition state analog bound in antibody 7A1 active site [28]. Residues TyrH50 and TyrL94 hydrogen bond to the phosphonate oxygen. Adapted from the crystal structure of antibody GNL7A1 complexed with the phosphonate transition state analog GNL (Protein Data Bank Accession code 2AJX, Zhu *et al*,[28]).

Table 1

Kinetic data for GNL mAbs that hydrolyze cocaine

MAb	k_{cat} (min^{-1})[a]	K_m (μM)	k_{cat}/K_m (M^{-1} s^{-1})	k_{cat}/k'_{uncat}[b]	Ref
GNL3A6	1.37×10^{-2}	53	4.35	1.36×10^{3}	29
GNL23A6	4.91×10^{-3}	430	0.183	4.86×10^{2}	29
GNL4D3	1.31×10^{-3}	42	0.517	1.30×10^{2}	29
GNL7A1	2.5×10^{-2}	750	0.556	2.63×10^{3}	28

[a] Reactions were carried out in 100 mM phosphate buffer, pH 7.4, with 5% DMSO cosolvent, at 23°C.

[b] $k'_{uncat} = 9.74 \times 10^{-6}$ min^{-1}, Zhu *et al.*[28]

Table 2

Kinetic data for GNL scFvs that hydrolyze cocaine

scFv	k_{cat} (10^{-4} min^{-1})[a]	K_m (mM)	k_{cat}/K_m (M^{-1} min^{-1})	k_{cat}/k'_{uncat}[b]
3F2	7.9 ± 1.9	0.40 ± 0.21	1.96	190
3F3	11.0 ± 0.8	0.30 ± 0.05	3.55	260
3F5	6.7 ± 0.4	0.38 ± 0.05	1.77	160
3H9	3.6 ± 0.6	0.57 ± 0.17	0.63	90

[a] Reactions were carried out in phosphate buffered saline, pH 7.4, at 23°C.

[b] $k'_{uncat} = 4.1 \times 10^{-6}$ min^{-1}

Table 3

Kinetic data for scFv 3F5 alanine mutants

scFv	k_{cat} (10^{-4} min^{-1})[a]	K_m (mM)	k_{cat}/K_m (M^{-1} min^{-1})	k_{cat}/k'_{uncat}[b]
wt	6.7 ± 0.4	0.38 ± 0.05	1.77	160
ProH53Ala	5.1 ± 1.0	0.46 ± 0.14	1.10	120
AspH57Ala	4.6 ± 0.3	0.63 ± 0.05	0.73	110
GlnH59Ala	9.1 ± 1.6	0.63 ± 0.20	1.44	220
GlnH62Ala	11.0 ± 0.2	0.47 ± 0.01	2.36	270
ThrH95Ala	8.1 ± 0.4	0.30 ± 0.03	2.70	200
GlnH97Ala	ND[c]			
HisH99Ala	ND			
HisL93Ala	8.8 ± 2.3	0.72 ± 0.32	1.22	210
HisL96Ala	ND			

[a] Reactions were carried out in phosphate buffered saline, pH 7.4, at 23°C.

[b] $k'_{uncat} = 4.1 \times 10^{-6}$ min^{-1}

[c] ND, not detectable.

Table 4

Kinetic data of scFv 3F3 and 3F4 mutants

scFv	k_{cat} (10^{-4} min^{-1})[a]	K_m (mM)	k_{cat}/K_m (M^{-1} min^{-1})	k_{cat}/k'_{uncat}[b]
3A6	11.4 ± 0.2	1.2 ± 0.1	0.93	280
3F3 wt	11.0 ± 0.8	0.3 ± 0.1	3.55	260
3F3 HisH50Tyr	23.6 ± 2.9	0.9 ± 0.2	2.62	580
3F3 HisH50Gln	30.6 ± 1.5	0.9 ± 0.1	3.38	750
3F3 HisH50Asn	ND[c]			
3F3 HisH50Arg	ND			
3F3 HisH50Gln,ArgH52Lys	83.5 ± 9.5	2.5 ± 0.6	3.34	2040
3F3 TyrL94His	7.4 ± 0.7	0.6 ± 0.1	1.20	180
3F4 wt	ND			
3F4 TyrH50His	1.4 ± 0.1	2.9 ± 0.7	0.05	30
3F4 TyrL94His	2.2 ± 0.2	4.5 ± 0.9	0.05	50
3F4 TyrH50His,TyrL94His	3.0 ± 0.2	1.3 ± 0.2	0.22	70

[a] Reactions were carried out in phosphate buffered saline, pH 7.4, at 23°C.

[b] $k'_{uncat} = 4.1 \times 10^{-6}$ min^{-1}

[c] ND, not detectable.